Observation of Higher-Harmonic Helical Spin-Resonance Modes in the Chromium Spinel $CdCr_2O_4$

S. Kimura,[1] M. Hagiwara,[1] H. Ueda,[2,3] Y. Narumi,[2] K. Kindo,[2] H. Yashiro,[1] T. Kashiwagi,[1] and H. Takagi[3,4]

[1]*KYOKUGEN, Osaka University, Machikaneyama 1-3, Toyanaka 560-8531, Japan*

[2]*Institute for Solid State Physics, The University of Tokyo, Kashinoha 5-1-5, Kashiwa 277-8581, Japan*

[3]*RIKEN (The Institute of Physical and Chemical Research), Hirosawa 2-1, Wako, Saitama 351-0198, Japan*

[4]*Department of Advanced Materials Science, The University of Tokyo, Hongo 7-3-1, Bunkyo, Tokyo 113-8656, Japan*

(Received 15 July 2005; revised manuscript received 4 August 2006; published 18 December 2006)

High frequency ESR measurements on the chromium spinel compound $CdCr_2O_4$ have been performed. The observed ESR modes below $H_c' \approx 5.7$ T can be explained well by the calculated resonance modes based on a molecular field theory assuming a helical spin structure. Other than the fundamental ones, we have succeeded in observing the higher-harmonic modes for the first time. A large change of the ESR modes above H_c' indicate that a variation of the spin structure from the helical to the four-sublattice canted one takes place around H_c'.

DOI: 10.1103/PhysRevLett.97.257202 PACS numbers: 75.10.Hk, 75.50.Ee, 76.50.+g

AB_2O_4 spinel compounds have attracted renewed interests because of very rich physical behavior caused by spin frustration. Magnetic ions on the B site of the spinel structure form a pyrochlore lattice, which is composed of a three-dimensional arrangement of corner sharing tetrahedra. Strong spin frustration arises in the pyrochlore lattice, when the nearest-neighbor exchange interaction is antiferromagnetic. It has been theoretically demonstrated that both $S = \infty$ classical and quantum $S = 1/2$ Heisenberg pyrochlore antiferromagnets do not order down to zero temperature, owing to vast degeneracy of the ground state [1–3]. However, some chromium spinel compounds are known to show a peculiar magnetic phase transition, which is explained in terms of the ''spin-driven Jahn-Teller effect''. The spin-lattice coupling plays an essential role for this phenomenon in relieving the geometrical frustration [4–8]. The magnetic phase transition in some chromium spinels is of first order, accompanied by a distortion of the crystal structure from a cubic to a lower symmetry one [4–7]. The degeneracy lifting is caused by lowering of the symmetry in the crystal lattice, resulting in inducing the magnetic order.

The chromium spinel $CdCr_2O_4$ undergoes the transition from a paramagnetic phase with a cubic symmetry to a magnetically ordered phase with a tetragonal one below $T_N = 7.8$ K. A helical spin structure was suggested to be realized in the ordered state from a recent neutron scattering measurement [9]. The magnetization measurements at low temperatures showed a very interesting behavior—that a $1/2$ magnetization plateau appears above $H_c \approx 28.5$ T [10]. The magnetization below H_c almost linearly increases with increasing magnetic field, but one can see a small anomaly at low fields $H_c' \approx 5.7$ T, accompanied by a hysteresis.

In this Letter, we report the observation of the magnetic excitation of $CdCr_2O_4$ by high field/high frequency ESR measurements. One remarkable new finding is an observation of higher-harmonic modes of the helical spin system. The observations of the novel magnetic excitation mode have often stimulated theoretical interests and opened new physics. From the 1960s, magnetic excitation of helical spin systems has been intensively studied. Strikingly different from the simple two-sublattice antiferromagnet with two excitation modes, the conventional spin wave theory showed three fundamental modes, which correspond to the ω_0 and $\omega_{\pm\phi}$ in our notation, for the helical spin system [11]. The theoretical results were successfully confirmed by neutron scattering measurements on some rare earth metals [11]. However, previous studies examined only these fundamental excitation modes. In this study, beyond the fundamental modes, we succeed in observing other high frequency excitation modes in the field region below H_c' and reasonably explaining them by the higher-harmonic modes. Furthermore, large changes of the ESR modes were found around H_c'. The ESR modes characteristic of the helical structure disappear around H_c', then those expected from the four-sublattice canted spin structure are observed above H_c'. This result suggests a peculiar behavior that the spin structure varies from the helical to the canted one around H_c'.

High field/high frequency ESR measurements on single crystal and powder samples of $CdCr_2O_4$ have been performed in the frequency region from 70 GHz to 1.4 THz. The measurements in the frequency region from 326 GHz to 1.4 THz under pulsed magnetic fields at 1.3 K were conducted by using a far-infrared laser as a light source. Detailed frequency dependence of the ESR spectrum below 360 GHz in static magnetic field up to 14 T at 1.6 K was measured by utilizing a vector network analyzer and a superconducting magnet. For the single crystal measurements, the magnetic field is applied parallel to the [100], [110], and [111] direction in cubic indices.

Figure 1(a) shows the frequency dependence of the ESR spectra of $CdCr_2O_4$ powder sample observed below

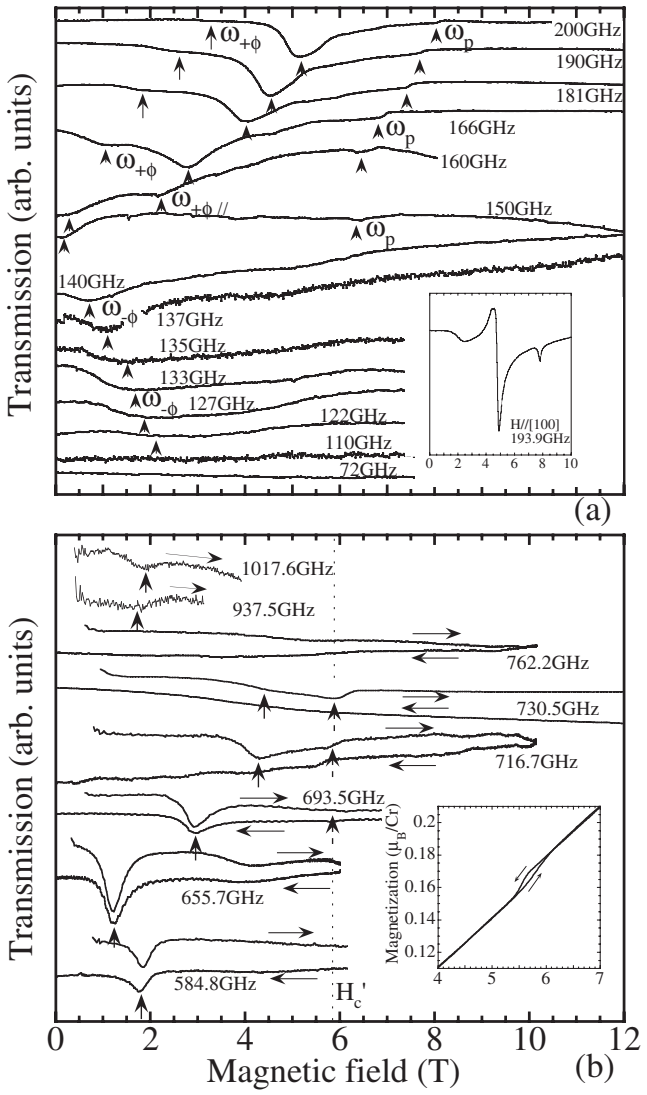

FIG. 1. (a) Frequency dependence of the ESR spectra observed in the powder sample below 200 GHz at 1.6 K. The inset shows the ESR spectrum observed in the single crystal for $H \parallel [100]$ at 193.9 GHz. (b) Frequency dependence of the ESR spectra in the single crystal for $H \parallel [100]$ in the frequency region from 580 to 760 GHz at 1.3 K. Dotted line shows H_c' observed in the field ascending process. The inset shows the magnetization curve for $H \parallel [100]$ observed under pulsed magnetic field at 1.3 K.

200 GHz. As shown in the inset of Fig. 1(a), rather complicated ESR spectra were observed in the single crystal, probably arising from multiple domains in the crystal lattice with a tetragonal symmetry below T_N. The observed spectrum is the overlap of the ESR absorption lines for the field applied to the several kinds of the crystal directions, and this makes difficult to determine ESR modes for field parallel to the magnetic principal axes. Thus, we measured the ESR spectra of the powder sample. The powder ESR spectra show some structures as indicated by arrows in Fig. 1(a). One can assign the resonance absorption fields for H parallel to the principal axes from such structures, because the edges or the maximum of the magnon density exist along the principle axes [12]. Three kinds of the ESR modes $\omega_{+\phi}$, $\omega_{-\phi}$ and $\omega_{+\phi\parallel}$ were observed for $H < H_c'$ at frequency below 300 GHz as shown in the inset of Fig. 2. The $\omega_{-\phi}$ mode, which shows a nonlinear field dependence with a negative slope, is very different from the ESR mode of a conventional two-sublattice antiferromagnet, and these modes can be well explained by the fundamental excitation modes of the helical spin system, as will be shown later. Furthermore, in addition to these fundamental modes, we find other ESR signals in the high frequency region as shown in Fig. 1(b). Figure 2 shows the frequency-field diagram of the ESR signals observed in the frequency region up to 1.2 THz. The high frequency ESR modes were found in the frequency region from 580 to 760 GHz and around 1000 GHz. The following molecular field calculation will reveal that these high frequency modes are reasonably interpreted by higher-harmonic modes characteristic of a helical spin system.

Next, we show the ESR modes for a helical spin system based on a molecular field theory. The origin of the helical structure is not clear at the moment, but an importance of further neighbor interactions has been suggested [9]. Recent theories [8,13], taking into account a tetragonal distortion, demonstrated that one of the stable spin structures of a pyrochlore antiferromagnet with the nearest-neighbor interactions is a collinear one represented by antiferromagnetic alignments of spins on the chains along

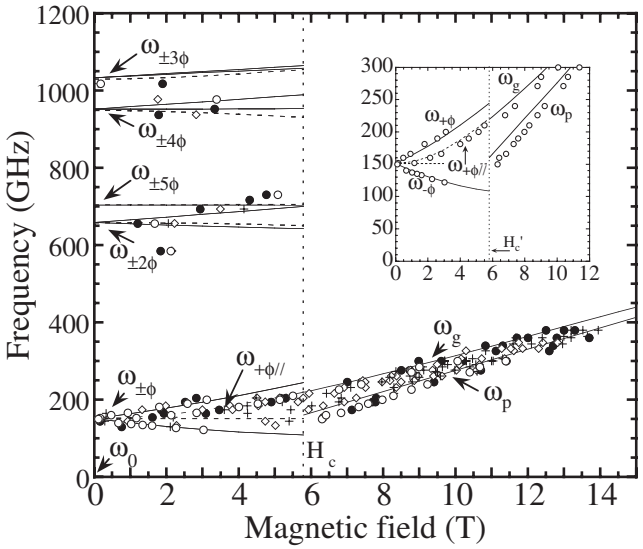

FIG. 2. Frequency-field relation of the ESR resonance points in $CdCr_2O_4$. Closed circles, open diamonds, and crosses represent these in the single crystal for $H \parallel [100]$, [110], and [111], respectively. The open circles represent those observed in the powder sample. Solid and dashed curves below H_c' shows the theoretical ESR modes assuming a helical structure for the field perpendicular and parallel to the easy plane, respectively. The solid curves above H_c' shows those of the two-sublattice model. Dotted vertical line shows H_c' observed in the field ascending process. The inset shows the extended figure below 300 GHz for the powder sample.

the [1, 1, 0] or [1, $\bar{1}$, 0] axis in the tetragonal c plane. In this structure, as molecular fields coming from the nearest-neighbor chains cancel each other, the magnetic properties are considered to be determined essentially by the interactions along the chain. In such a case, if the next-nearest intrachain interaction is sufficiently large compared with that between the nearest ones, the helical structure is probably realized because a competition between the interactions makes the collinear structure unstable. We assume a helical structure with a modulation wave number $q = 0.1$, which corresponds to a ten-sublattice structure with a pitch angle $\phi = 108°$, as depicted in Figs. 3(a)–3(c). On the other hand, the spin structures, proposed from the neutron diffraction measurement, were incommensurate ones, characterized by an ordering vector $\boldsymbol{Q} = (0, \delta, 1)$ with $\delta \approx 0.09$ [9]. However, the spin structure has not been uniquely determined, and the helical spin structures with a phase difference of $\phi = 171.8°$ [9] between the nearest-neighbor spins, which is different with that assumed in our ESR analysis, were deduced in Ref. [9]. The spin wave energies strongly depend on the angle ϕ, and the excitation modes, calculated from the angle given in Ref. [9], are incompatible with the observed ESR modes. The molecular field energy of our model is expressed as follows:

$$E = A\sum_j \boldsymbol{M}_j\boldsymbol{M}_{j+1} + B\sum_j \boldsymbol{M}_j\boldsymbol{M}_{j+2} + \frac{1}{2}\sum_j \boldsymbol{M}_j\tilde{\Gamma}'\boldsymbol{M}_j - \boldsymbol{H}\sum_j \boldsymbol{M}_j \quad (1)$$

and

$$\tilde{\Gamma}' = \begin{pmatrix} \Gamma' & 0 & 0 \\ 0 & \Gamma' & 0 \\ 0 & 0 & -2\Gamma' \end{pmatrix}, \quad (2)$$

where the first and the second term show the nearest and the next-nearest interaction, respectively, and the third term represents the easy plane type anisotropy. $\boldsymbol{M}_j$ corresponds to the jth sublattice moment. When a condition $A < 4B$ is satisfied, the helical structure is stable at zero field. The pitch angle ϕ of the helical structure is given by $\cos\phi = -A/4B$. As mentioned above, only three kinds of the fundamental excitation modes ω_0 and $\omega_{\pm\phi}$ have been examined for a helical spin system based on a spin wave theory so far [11]. However, when we treat the system with ten sublattice, ten kinds of the normal modes $\omega_{n\phi}$ ($n = 0$, ±1, ±2, ±3, ±4, 5) exist. We derive the resonance conditions for all of the normal modes, according to the conventional method by solving the equation of motion: $\partial\boldsymbol{M}_j/\partial t = \gamma[\boldsymbol{M}_j \times \boldsymbol{H}_j]$, where γ is the gyromagnetic ratio, $\boldsymbol{H}_j$ is a mean-field acting on the jth sublattice, given by $\boldsymbol{H}_j = -\partial E/\partial\boldsymbol{M}_j$. When the external field is applied perpendicular to the easy plane, an umbrella structure shown in Fig. 3(b) is realized. The angle θ between each individual magnetic moment and field is given in the literature [11]. Assuming precession motions of the sublattice moments around those equilibrium directions, the equations of motion can be solved by substitutions of the following expressions, which represent the motion of the jth sublattice moment,

$$M_j^x = \Delta M\cos(\omega t + n\phi j), \quad (3)$$

$$M_j^y = \lambda\Delta M\sin(\omega t + n\phi j). \quad (4)$$

The $n\phi$ gives a phase deference of the precession motions between adjacent sublattices. Here, the x and the y directions are defined to be perpendicular to the equilibrium direction of the magnetization of each sublattice. ΔM and λ are constants and n is integer of $n = 0, \pm1, \pm2, \pm3, \pm4$, 5. We define the normal mode of $n = i$ to be $\omega_{i\phi}$. ω_0 and $\omega_{\pm\phi}$ correspond to the fundamental modes $\omega(0)$ and $\omega(\pm k_0)$, which were given by the previous spin wave calculation [11]. For a field parallel to the easy plane, we assume the distorted structure, depicted in Fig. 3(c), in which spins are lying in the easy plane. The conditions $\phi_1 = \phi_4$, $\phi_2 = \phi_3$, $\phi_5 = \phi_{10}$, $\phi_6 = \phi_9$, and $\phi_7 = \phi_8$ are assumed, where ϕ_j represents an angle between the jth sublattice and the magnetic field. The angles ϕ_j's are determined so as to minimize the energy of the assumed structure by solving differential equations $-\partial E/\partial\phi_j = 0$ ($j = 1, 2, 5, 8, 9$). Since analytical expressions of the resonance conditions are difficult to be obtained owing to the distortion of the spin structure, we acquire the resonance conditions by numerical solution of the equations of motion.

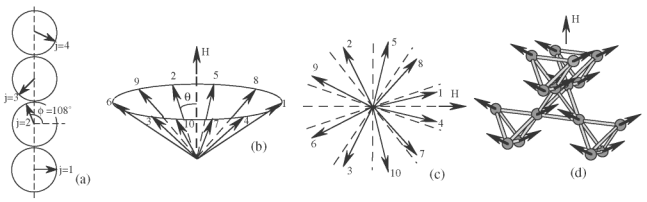

FIG. 3. The helical spin structure with pitch angle $\phi = 108°$ (a). The spin structure under magnetic field perpendicular to the easy plane (b) and that for field parallel to the easy plane (c). The canted spin structure, which gives the AFMR modes observed for $H > H_c'$ (d).

As shown in the inset of Fig. 2, the ESR modes, observed in the frequency region below 300 GHz for $H < H_c'$, are explained by the fundamental resonance modes for the helical spin system, calculated with the exchange fields $H_{E1} = AM_0 = 18.0$ T, $H_{E2} = BM_0 = 14.6$ T, the anisotropy field $H_A = 3\Gamma' M_0 = 0.503$ T, and $g = 1.97$. Here, M_0 is the magnitude of the sublattice magnetization. Solid and dashed curves for $H < H_c'$ in Fig. 2 are the theoretical curves for fields perpendicular and parallel to the easy plane, respectively. By these parameters the pitch angle $\phi = 108°$ is reproduced. The results of our calculation, that the frequency of the ω_0-mode remains zero, namely, a gapless mode in finite fields, both for perpendicular and

parallel to the easy plane, are consistent with the previous spin wave calculations [11]. The higher-harmonic modes $\omega_{n\phi}$ of $n \geq 2$ are calculated with the same parameters. As shown in Fig. 2, the observed high frequency ESR modes are reasonably explained by the theoretical modes of $n \geq 2$. It should be mentioned that the resonance modes, showing very small field dependence, such as $\omega_{5\phi}$, can hardly be observed by the conventional ESR measurement, namely, the field sweeping measurement. To check the above parameters, a magnetic susceptibility $\chi_{\text{calc}} = (1/3)\chi_{\perp} + (2/3)\chi_{\parallel}$ of the powder sample is calculated. The $\chi_{\perp}$ and $\chi_{\parallel}$ represent the susceptibilities for field perpendicular and parallel to the easy plane. They can be obtained from the angles θ and ϕ_j. The calculated susceptibility $\chi_{\text{calc}} = 0.0299$ emu/mol is not far from the experimental result $\chi_{\text{exp}} = 0.0212$ emu/mol, observed at 0.1 T and 2.0 K. The reduction of χ_{exp} possibly reflects the spin fluctuation, observed by a previous μSR measurement [6].

To our knowledge, this is the first time that the higher-harmonic modes for the helical spin system have been satisfactorily observed. For the normal modes other than the ω_0 and $\omega_{\pm\phi}$, the total magnetization is not in motion because time dependent parts of the sublattice moments cancel each other. Therefore, these modes are, in principle, not observable. However, the situation probably changes if phonons are taken into account. Several mechanisms for phonon assisted optical magnon absorption have been proposed theoretically. These are not only an excitation due to the magnon virtual bound state assisted by phonon [14], which will require an energy much larger than the one for a single magnon excitation, but also a transition via a creation of a virtual phonon [15]. We speculate that owing to the strong spin-lattice coupling in $CdCr_2O_4$ [10], the phonon, which effectively lowers the symmetry of the system, is possible to play a crucial role to give finite transition probabilities for the normal modes $\omega_{n\phi}$ of $n \geq 2$. We hope these experimental results and our speculation stimulate further detailed theory.

Finally, we discuss drastic change of the ESR modes, seen around $H_c' \approx 5.7$ T. With increasing resonance field, the intensities of the ESR signals $\omega_{+\phi}$ and $\omega_{-\phi}$ decrease and these ESR signals disappear above H_c', whereas a new ESR signal ω_p appears near the resonance field of $g = 1.97$ around H_c', as shown in Fig. 1(a). The ESR signals of the higher-harmonic modes, shown in Fig. 1(b), also decrease those intensities with increasing resonance field and disappears above H_c'. Moreover, these ESR signals show hysteretic behaviors. The intensity of the ESR signals in the field-descending process is observed to be weaker than that in the ascending one. The frequency-field relation, as shown in Fig. 2, indicates that the ESR modes characteristic of a helical spin structure disappear around H_c', whereas the ESR modes ω_g and ω_p, which appear near the paramagnetic resonance line of $g = 1.97$, are observed above H_c'. The ESR modes ω_p and ω_g can be explained by the theoretical equations $\omega_p/\gamma = H$ and $\omega_g/\gamma = \sqrt{H^2 + E_g^2}$ with $E_g = 150$ GHz, respectively. These equations correspond to the antiferromagnetic resonance (AFMR) modes of the conventional two-sublattice model with easy plane anisotropy [16]. One of the spin structures, which gives such AFMR modes, is the canted spin structure, depicted in Fig. 3(d). Since this structure is expressed by the four-sublattice model, four kinds of AFMR modes are expected. However, the AFMR modes other than the above are not observable. Our experimental results suggest that a variation of the spin structure from a helical to a canted one occurs around H_c'. As seen in the magnetization process and the ESR signals, this phenomenon is accompanied by the hysteresis. Such behaviors, however, cannot be explained within the framework of our molecular field model. On the other hand, a small anomaly of the baseline of the ESR spectrum, which corresponds to a change of amplitude of transmitted light through the sample, is seen at H_c', as indicated by dashed arrows in Fig. 1(b). This suggests a change of the dielectric constant at H_c'. We consider that the change is caused by some transformation of the crystal lattice. If the lattice transformation relaxes the competition between the nearest and the next-nearest interactions, the variation of the spin structure from a helical to a canted one is possible to take place, and the lattice transformation might require some relaxation time giving rise to the hysteresis.

The authors are grateful to Dr. M. Matsuda of the Japan Atomic Energy Research Institute for showing us his experimental results prior to publication and for valuable comments. This work was partly supported by Grant-in-Aid for Science Research on Priority Areas from the Japanese Ministry of Education, Science, Sports, Culture and Technology.

[1] J. Villlain *et al.*, Z. Phys. B **33**, 31 (1979).
[2] R. Moessner and J. T. Chalker, Phys. Rev. B **58**, 12 049 (1998).
[3] B. Canals and C. Lacroix, Phys. Rev. B **61**, 1149 (2000).
[4] Y. Kino and B. Luthi, Solid State Commun. **9**, 805 (1971).
[5] R. Plumier *et al.*, J. Phys. Lett. **38**, L149 (1977).
[6] M. T. Rovers *et al.*, Phys. Rev. B **66**, 174434 (2002).
[7] S.-H. Lee *et al.*, Phys. Rev. Lett. **84**, 3718 (2000).
[8] O. Tchernyshyov *et al.*, Phys. Pev. B **66**, 064403 (2002).
[9] J.-H. Chung *et al.*, Phys. Rev. Lett. **95**, 247204 (2005).
[10] H. Ueda *et al.*, Phys. Rev. Lett. **94**, 047202 (2005).
[11] B. R. Cooper, *Magnetic Properties of Rare Earth Metals*, Solid State Physics Vol. 21 (Academic, New York, 1968), p. 393, and references therein.
[12] H. Ohta *et al.*, J. Phys. Soc. Jpn. **61**, 149 (1992).
[13] K. Terao, J. Phys. Soc. Jpn. **65**, 1413 (1996).
[14] J. Lorenzana and G. A. Sawatzky, Phys. Rev. Lett. **74**, 1867 (1995).
[15] O. Cépas *et al.*, Phys. Rev. Lett. **87**, 167205 (2001).
[16] T. Nagamiya *et al.*, Adv. Phys. **4**, 1 (1955).